

# Electromechanical properties of 1-3 piezoelectric ceramic/piezoelectric polymer composites

H. Taunamang<sup>a)</sup> and I. L. Guy

School of Mathematics, Physics, Computing, and Electronics, Macquarie University,  
New South Wales 2109, Australia

H. L. W. Chan

Department of Applied Physics, Hong Kong Polytechnic, Hung Hom, Kowloon, Hong Kong

(Received 17 September 1993; accepted for publication 10 March 1994)

A study of the fabrication and electromechanical properties of piezoelectric 1-3 ceramic/polymer composites is reported in which the polymer phase, as well as the ceramic phase, is piezoelectric. Composites were prepared by both layering and dice-and-fill techniques. In the dice-and-fill technique, the major problem was preventing damage to the ceramic rods during the filling process. Both types of composite were found to present problems in the poling process. The electromechanical properties of the composites were measured and compared with modeling results. In general, it was found that the composite properties agreed with model predictions, with the exception of the piezoelectric coefficients, which were significantly lower than predicted.

## I. INTRODUCTION

Recently, 1-3 composites (shown schematically in Fig. 1) have proven to be useful materials for medical ultrasonic transducer<sup>1,2</sup> and underwater hydrophone<sup>3</sup> applications because they have lower acoustic impedance and higher electromechanical coupling than conventional piezoceramics. 1-3 composites are usually composed of piezoelectric ceramics and nonpiezoelectric polymers. The present work involved the investigation of 1-3 ceramic/polymer composites in which both ceramic and polymer phases are piezoelectric. This material, if properly designed, is expected to provide useful new properties for ultrasonic transducer applications. For example, the composite with two piezoelectric phases can be used to fabricate novel structure transducers such as two intertwined arrays using the ceramic phase to transmit and using the piezopolymer matrix to receive. In addition the interaction of the piezoelectric effect in the two phases presents interesting possibilities. The piezoelectric coefficients of the ceramic and polymer are of opposite signs and thus tend to cancel in the  $d_{33}$  and  $d_{31}$  of the composite. Since the coercive fields of the two phases are significantly different, it may be possible to pole the two phases in opposite directions, giving a composite in which the contributions of  $d_{33}$  and  $d_{31}$  add. However, the hydrostatic coefficient comes about by an addition of  $d_{31}$ ,  $d_{32}$ , and  $d_{33}$ . In producing the hydrostatic coefficient of the composite, the contributions from the ceramic  $d_{31}$  and the polymer  $d_{33}$  add, while the contributions of the ceramic  $d_{33}$  and polymer  $d_{31}$  subtract.<sup>4</sup> The relative magnitude of the effects will depend crucially on the mechanical anisotropy of the polymer phase. This means that in the design of the composite it would be possible to choose to enhance  $d_{33}$  or  $d_h$ .

The polymer used in the present work was a 75/25 mol % copolymer of vinylidene fluoride (VDF or VF<sub>2</sub>) and trifluoroethylene (TrFE), obtained from Solvay et Cie of Bel-

gium. The ceramic used was TLZ-5 (equivalent to PZT-5H from Vernitron) from GEC-Marconi, Australia. The homopolymer polyvinylidene fluoride (PVDF) normally crystallizes in a nonpolar  $\alpha$  crystal form and needs mechanical stretching to convert it into a polar  $\beta$  form for piezoelectric applications. The copolymer has been found to spontaneously crystallize in the  $\beta$  form<sup>5</sup> if the TrFE content is above about 20 mol %, hence avoiding the need for stretching. Casting from acetone was found to be a suitable method for incorporating the polymer into the composites. The composite properties were measured and compared with predictions based on Smith's model.<sup>6</sup>

## II. SAMPLE PREPARATION

The 1-3 composites were produced by the dice-and-fill<sup>7</sup> and the lamination<sup>8</sup> methods. In the dice-and-fill method, two sets of closely spaced, parallel cuts were made in a TLZ-5 disk, the two sets being perpendicular to each other. A total of 12 ceramic disks were diced, six were diced at the Macquarie University workshop with a saw blade of 0.5 mm thickness, another six disks were diced by AWA Pty. Ltd., using a blade with a cut width of 100  $\mu$ m. In order to fill the grooves in the disk with copolymer, each diced ceramic disk was placed in turn in a glass petri dish and a solution of

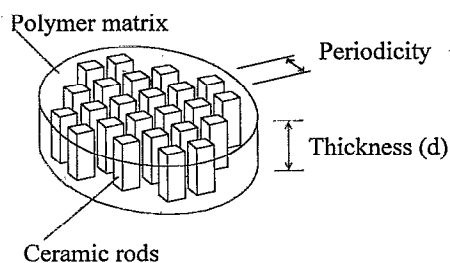


FIG. 1. Schematic diagram of a 1-3 composite, illustrating the ceramic rods embedded in a polymer matrix. The rods extend through the full thickness of the composite.

<sup>a)</sup>Present address: FDMIPA, Ikip Manado di Tonsaru, Sulawesi Utara, Manado, Indonesia 95115.

TABLE I. 1-3 TLZ-5/VDF/TrFE copolymer composites.

Ceramic width (mm)	Periodicity (mm)	Thickness (mm)	Density $\rho$ ( $\text{kg m}^{-3}$ )	Vol. fraction ceramic
Composites produced by the dice-and-fill process				
0.33	0.49	0.90	4588	0.45
0.61	0.73	1.31	5792	0.65
0.98	1.10	1.33	6694	0.80
Composites produced by the lamination process				
0.87	1.7	0.7	3010	0.26
0.75	1.2	2.2	3840	0.40

copolymer poured over the disk. Bubbles which were trapped in the grooves were removed by running a fine wire through the grooves, while observing the sample under a microscope. Acetone was routinely used as the solvent for the copolymer since this solvent produced the least significant residual effects.<sup>9</sup> The samples were left for 5 days at room temperature, thus allowing the solvent to evaporate as slowly and completely as possible. The composites were then annealed at 120 °C for 2 h in order to increase the polymer crystallinity and to reduce the possibility of pinhole defects. Final finishing of the composite to the desired thickness was done by lapping, using abrasive papers of various grades.

Several problems were encountered during the processing of the composites and the final yield of successful dice-and-fill composites was only three (Table I) from the initial 12 diced disks. The main difficulty encountered which was responsible for the loss of most samples was the shrinking of the copolymer in the final stages of solvent evaporation. This shrinking caused the thin ceramic rods to break and be pulled inward and was most serious in the finer scale samples. Various methods, such as slowing down the evaporation rate or filling the grooves in stages were tried, however, no method was found which would completely overcome the problem.

Two 1-3 composites were prepared (Table I) by the lamination (or layering) method.<sup>8</sup> 1-mm-thick TLZ-5 rectangular plates were used. Pieces of copolymer of various thickness were cut from commercial sheet and stacked, interleaved with the ceramic plates. The layers were glued together using a thin film of epoxy (Araldite 38-204). The stack of layers thus formed was sliced, using a diamond saw, then reglued with additional polymer layers. This second stack was sliced again to produce thin composite sheets.

The composites were poled by corona poling.<sup>10</sup> Poling of the composites presented problems because of the high poling field required by the copolymer. The ceramic poling field is typically 5 kV mm<sup>-1</sup> while that for the copolymer is 50 kV mm<sup>-1</sup>. It was found that breakdown occurred in the samples at fields below the poling field of the copolymer. This breakdown occurred at the interface between the ceramic and the copolymer phases. The onset of breakdown limited the poling field which could be achieved to 5–10 kV mm<sup>-1</sup>. This field was applied for 30 min at room temperature.

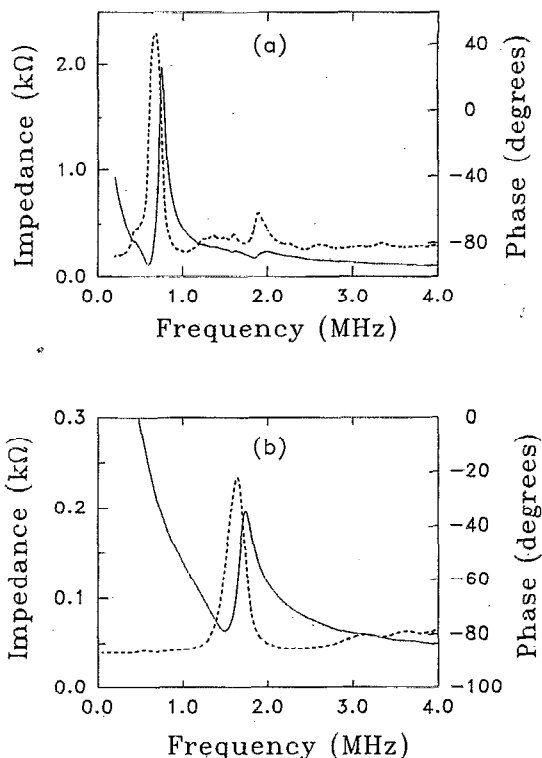


FIG. 2. Plots of electrical impedance (solid curves) and phase angle (dotted curves) vs frequency for 1-3 TLZ-5/copolymer composites: (a) with 0.4 volume fraction ceramic and 2.2 mm thickness; (b) with 0.26 volume fraction ceramic and 0.3 mm thickness.

### III. MEASURED PROPERTIES OF THE 1-3 COMPOSITES

Elastic constants were evaluated from measurements of the velocities of longitudinal and shear waves in the composite using the immersion method.<sup>11</sup> Electromechanical properties of the composites were measured from the electrical impedance resonance. Impedance versus frequency curves for two of the composites are shown in Fig. 2. Values of  $k_t$  were calculated as described in the IEEE standard on piezoelectricity.<sup>12</sup>

The hydrostatic charge coefficient  $d_h$  was measured dynamically in a hydrostatic chamber,<sup>13</sup> made from polyvinyl chloride (PVC) and having dimensions of 15×15×7.5 cm<sup>3</sup>. Acoustic pressure was generated in the chamber by two loudspeakers, mounted on opposite faces as shown in Fig. 3. A grounded, brass gauze shield was placed around the sample in order to eliminate electromagnetic coupling of the

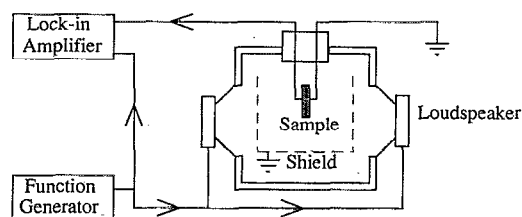


FIG. 3. Experimental setup for  $d_h$  measurement.

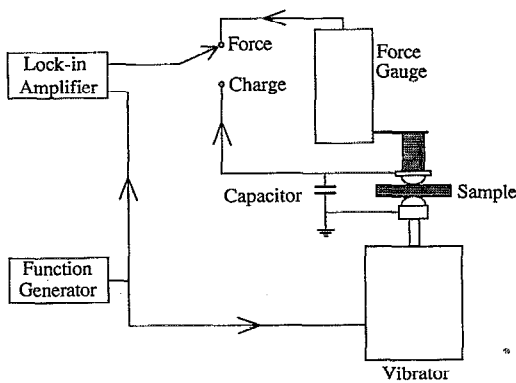


FIG. 4. Experimental setup for  $d_{33}$  measurement.

signal from the loudspeakers. The loudspeakers were driven by a function generator (HP 8116A) and measurements were normally carried out at a frequency of 80 Hz. This frequency is low enough to ensure that there is no significant spatial variation of acoustic pressure inside the chamber. The pressure inside the chamber was measured using a calibrated microphone (Brüel & Kjaer, type 4144). The piezoelectric voltage generated by the sample was measured by a lock-in amplifier (Princeton 5209) and the total capacitance of the sample plus the measurement system was measured with a General Radio 1615-A precision capacitance bridge. The piezoelectric charge generated by the sample was calculated from the measured piezoelectric voltage and the capacitance. A PZT-5A piezoelectric standard, in the form of a 1 cm cube, was used to check the calibration of the system.

The piezoelectric coefficient  $d_{33}$  was measured in a custom-built rig, illustrated in Fig. 4. A Ling model 201 vibrator was used to apply a sinusoidal stress to the sample and the resulting charge measured in the same way as for the  $d_h$  measurements. The force applied to the sample was measured by a Harvard model 373 force gauge. The PZT-5A standard cube was also used to calibrate this system.

#### IV. COMPARISON BETWEEN MODELING AND EXPERIMENTAL RESULTS

The modeling approach used by Smith<sup>6</sup> was followed, with a modification of the polymer crystal group. Since the VDF/TrFE copolymer crystallizes spontaneously in the piezoelectric form and does not need to be stretched, this leaves the copolymer isotropic in the 1-2 plane (plane of the sample disks) and leads to a 6 mm symmetry for the polymer.

The composite is assumed to be in the form of a thin plate, with lateral dimensions much larger than the separation between elements. Conducting electrodes are deposited on both surfaces of the plate. The  $x$  and  $y$  axes lie in the plane of the plate, while the  $z$  axis is perpendicular to it. In the following, the  $x$ ,  $y$ , and  $z$  axes are referred to by subscripts 1, 2, and 3, respectively. The symbols used conform to the nomenclature used in the IEEE piezoelectric standard,<sup>12</sup> namely  $T$  is stress,  $S$  is strain,  $E$  is electric field,  $D$  is electric displacement,  $c$  is elastic stiffness constant,  $s$  is elastic compliance,  $d, e$  are piezoelectric coefficients,  $k$  is the electromechanical coupling factor,  $\epsilon$  the electric permittivity, and  $\rho$  the density.  $V$  represents the acoustic velocity while  $\nu$  represents volume fraction. Superscripts  $P$  and  $C$  refer to the state variables of polymer or ceramic respectively. Superscripts  $D, S, T,$  and  $E$  are used for those properties of the piezoelectric ceramic and copolymer for which the particular state variable is held constant. A bar above a symbol represents a composite property, while an asterisk denotes a ceramic property. The resulting equations for composite properties are summarized as follows:<sup>6,14</sup>

$$\bar{\rho} = \rho^C \nu + \rho^P \nu, \quad (1)$$

$$\bar{k}_t = \frac{\bar{e}_{33}}{(c_{33}^D \bar{\epsilon}_{33}^S)^{0.5}}, \quad (2)$$

$$\bar{e}_{33} = \nu e_{33} + \nu^* e_{33}^* - 2 \left( \frac{\nu e_{31} c_{13}^E (c_{11}^E + c_{12}^E) + \nu^* e_{31}^* c_{13}^E (c_{11}^E + c_{12}^E)}{(c_{11}^E + c_{12}^E)(c_{11}^E + c_{12}^E)} \right) + 2 \left( \frac{[\nu e_{31} (c_{11}^E + c_{12}^E) + \nu^* e_{31}^* (c_{11}^E + c_{12}^E)] [\nu c_{13}^E (c_{11}^E + c_{12}^E) + \nu^* c_{13}^E (c_{11}^E + c_{12}^E)]}{(c_{11}^E + c_{12}^E)(c_{11}^E + c_{12}^E) [\nu (c_{11}^E + c_{12}^E) + \nu^* (c_{11}^E + c_{12}^E)]} \right), \quad (3)$$

$$\bar{e}_{33}^S = \nu e_{33}^S + \nu^* e_{33}^{*S} - 2 \left( \frac{\nu e_{31}^2 (c_{11}^E + c_{12}^E) + \nu^* e_{31}^{*2} (c_{11}^E + c_{12}^E)}{(c_{11}^E + c_{12}^E)(c_{11}^E + c_{12}^E)} \right) - 2 \left( \frac{[\nu e_{31} (c_{11}^E + c_{12}^E) + \nu^* e_{31}^* (c_{11}^E + c_{12}^E)]^2}{(c_{11}^E + c_{12}^E)(c_{11}^E + c_{12}^E) [\nu (c_{11}^E + c_{12}^E) + \nu^* (c_{11}^E + c_{12}^E)]} \right), \quad (4)$$

$$\bar{c}_{33}^D = \bar{c}_{33}^E + \frac{(\bar{e}_{33})^2}{\bar{\epsilon}_{33}^S}, \quad (5)$$

$$\bar{V}_3^D = \left( \frac{\bar{c}_{33}^D}{\bar{\rho}} \right)^{0.5}, \quad (6)$$

$$\bar{c}_{33}^E = \frac{2[\nu c_{13}^E (c_{11}^E + c_{12}^E) + \nu^* c_{13}^E (c_{11}^E + c_{12}^E)]^2}{(c_{11}^E + c_{12}^E)(c_{11}^E + c_{12}^E)[\nu(c_{11}^E + c_{12}^E) + \nu^*(c_{11}^E + c_{12}^E)]} - 2 \left( \frac{\nu(c_{11}^E + c_{12}^E)(c_{13}^E)^2 + \nu^*(c_{11}^E + c_{12}^E)(c_{13}^E)^2}{(c_{11}^E + c_{12}^E)(c_{11}^E + c_{12}^E)} \right) + \nu c_{33}^E + \nu^* c_{33}^E, \quad (7)$$

$$\bar{d}_h = \bar{d}_{33} + 2\bar{d}_{31}, \quad (8)$$

$$\bar{d}_{33} = \frac{\nu d_{33} s_{33}^E + \nu^* d_{33} s_{33}^E}{\nu s_{33}^E + \nu^* s_{33}^E}, \quad (9)$$

$$\bar{d}_{31} = \frac{\nu(d_{31} s_{33}^E - d_{33} s_{13}^E)}{s_{33}^E} + \frac{\nu^*(d_{31} s_{33}^E - d_{33} s_{13}^E)}{s_{33}^E} + \frac{(\nu d_{33} s_{33}^E + \nu^* d_{33} s_{33}^E)(\nu s_{13}^E s_{33}^E + \nu^* s_{13}^E s_{33}^E)}{s_{33}^E s_{33}^E (\nu s_{33}^E + \nu^* s_{33}^E)}, \quad (10)$$

$$\bar{\epsilon}_{33}^T = \frac{\nu(\epsilon_{33}^T s_{33}^E - d_{33}^2)}{s_{33}^E} + \frac{\nu^*(\epsilon_{33}^T s_{33}^E - d_{33}^2)}{s_{33}^E} + \frac{(\nu d_{33} s_{33}^E + \nu^* d_{33} s_{33}^E)^2}{s_{33}^E s_{33}^E (\nu s_{33}^E + \nu^* s_{33}^E)}, \quad (11)$$

$$\bar{Z} = (\bar{\rho} \bar{c}_{33}^D)^{0.5}. \quad (12)$$

Materials parameters of the ceramic and copolymer used in the calculations are shown in Table II. The values without a reference number were measured in the course of the present work, using the methods described in the previous section. Study of properties of thick copolymer films cast from solution<sup>9</sup> has shown that such films have a tendency to break down at lower poling fields. Hence the samples cast from acetone were poled using 26 kV mm<sup>-1</sup> while the commercial copolymer films from Solvay were poled using 51 kV mm<sup>-1</sup>. The latter figure is close to the switching field for the copolymer, as determined from polarization hysteresis loops.<sup>20</sup> Comparison between calculated values and measured values for the TLZ-5/copolymer composites are plotted in Figs. 5(a)–5(g). Values of the piezoelectric constants  $d_{33}$  and  $d_h$  of the copolymer depend strongly on poling field (Table III). The highest value of  $d_{33}$  ( $= -29.6$  pC N<sup>-1</sup>), measured in the film poled at 51 kV mm<sup>-1</sup>, is similar to the

published value from other authors.<sup>16</sup> In the model calculation, the value of  $-29.6$  pC N<sup>-1</sup> was used and this gives the upper limit of what can be expected. If the values of piezoelectric constants for the copolymer, corresponding to lower poling fields, are used to calculate the theoretical curves in Fig. 5, then the curves shift by no more than a few percent, however it needs to be recognized that the poling process affects other polymer properties as well as the piezoelectric coefficients. The implications of this for the plots in Fig. 5 has not been explored. From the graphs, it can be seen that measured parameters of the 1-3 composites agree quite well to those predicted by the model with the obvious exception of the piezoelectric coefficient  $d_h$ . For reasons which are not fully understood, the measured values of  $d_h$  are significantly lower than those predicted by the model. In fact the experimental values are much lower even than the model values predicted with zero piezoelectric contribution from the polymer phase.

It is noted that the value of  $k_r$  is enhanced over that of the individual phases and is close to the  $k_{33}$  value ( $=0.75$ ) for the ceramic. In effect the polymer phase, whether piezoelectric or not, does not apply much clamping to the rigid ceramic phase, which in turn acts almost as a series of freely vibrating rods. Some attempts were made to measure  $d_{33}$  for the composites; however the values obtained varied widely, apparently because sometimes mechanical contact coincided with a ceramic rod and sometimes with a polymer region. With finer scale samples it may be possible to perform this measurement.

TABLE II. Parameters of the ceramic and copolymer used in the model calculations. (The meaning of the symbols is given in Ref. 12.)

Parameter	TLZ-5	VDF/TrFE copolymer	Unit
$c_{11}^E$	126 <sup>a</sup>	8.5	GPa
$c_{12}^E$	79.5 <sup>a</sup>	3.6	GPa
$c_{13}^E$	84.1 <sup>a</sup>	3.6	GPa
$c_{33}^E$	109	9.9	GPa
$c_{33}^D$	147	10.7	GPa
$s_{11}^E$	17.4	154.9	(10 <sup>12</sup> Pa) <sup>-1</sup>
$s_{12}^E$	-4.1	-49.2	(10 <sup>12</sup> Pa) <sup>-1</sup>
$s_{13}^E$	-10.2	-38.9	(10 <sup>12</sup> Pa) <sup>-1</sup>
$s_{23}^E$	-8.45	-38.9	(10 <sup>12</sup> Pa) <sup>-1</sup>
$s_{33}^E$	24.9	130.6	(10 <sup>12</sup> Pa) <sup>-1</sup>
$e_{33}$	24.8	-0.29	C m <sup>-2</sup>
$e_{31}$	-6.5 <sup>b</sup>	0.008 <sup>c</sup>	C m <sup>-2</sup>
$d_{31}$	-269	9.4	pC N <sup>-1</sup>
$d_{33}$	746	-29.6	pC N <sup>-1</sup>
$\epsilon_{33}^S/\epsilon_0$	1813	6.0 <sup>d</sup>	
$\epsilon_{33}^D/\epsilon_0$	4200	9.0	
$\rho$	7898	1880	kg m <sup>-3</sup>
$k_r$	0.51	0.2	
$k_{33}$	0.75 <sup>b</sup>	0.116 <sup>c</sup>	
$k_p$	0.64 <sup>c</sup>	...	
$V_3^D$	4300	2385	ms <sup>-1</sup>
$d_h$	210	-10.9	pC N <sup>-1</sup>

<sup>a</sup>See Ref. 18.

<sup>b</sup>See Ref. 19.

<sup>c</sup>See Ref. 15.

<sup>d</sup>See Ref. 16.

<sup>e</sup>See Ref. 17.

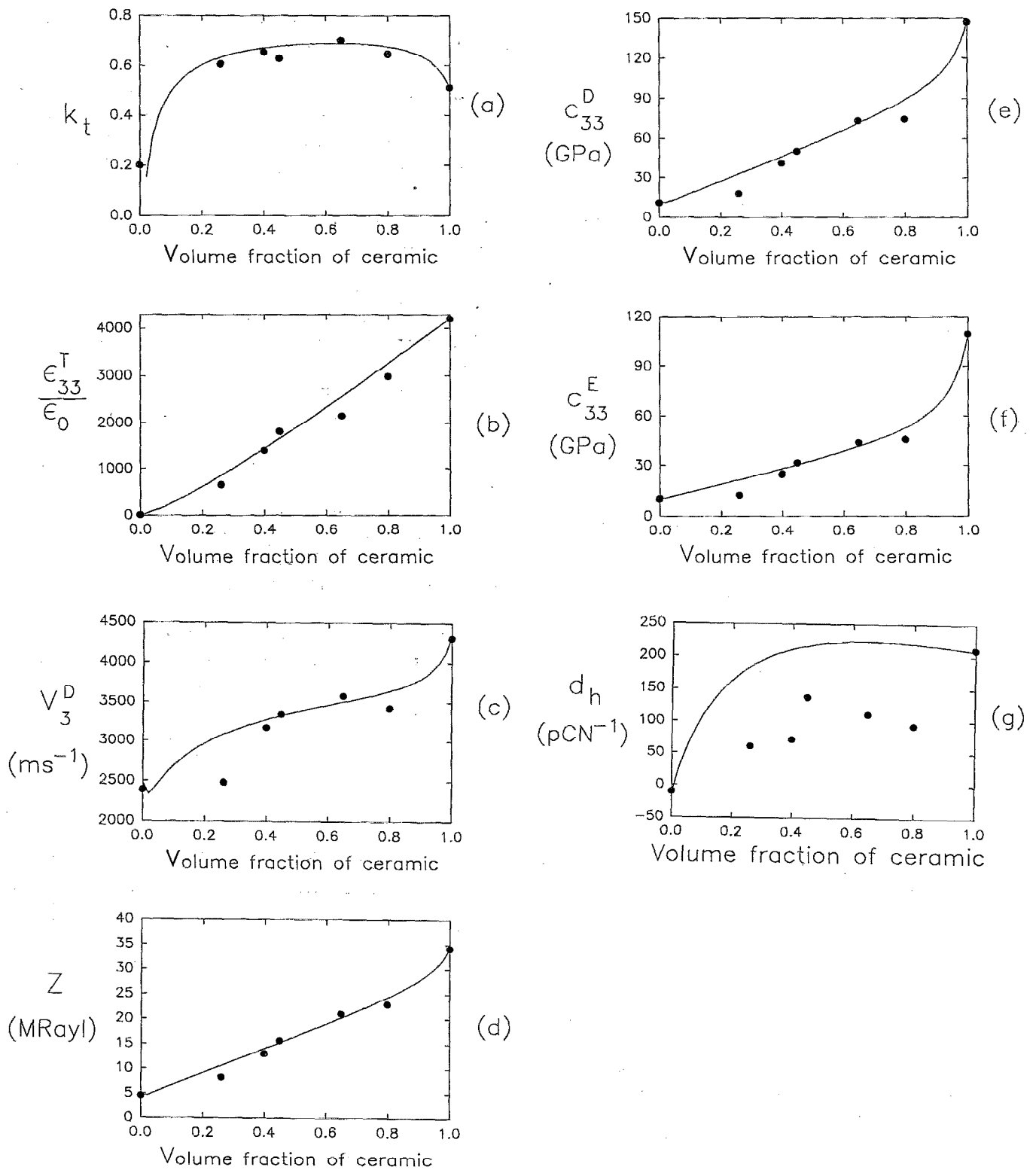


FIG. 5. Comparison between model predictions (solid line) and measured values (dots) of TLZ-5/copolymer composite properties as a function of ceramic volume fraction: (a) electromechanical coupling constant  $k_t$ ; (b) dielectric constant  $\epsilon_{33}^T/\epsilon_0$ ; (c) stiffened longitudinal velocity  $V_3^D$ ; (d) acoustic impedance  $Z$ ; (e) open-circuit stiffness constant  $c_{33}^D$ ; (f) short-circuit stiffness constant  $c_{33}^E$ ; (g) hydrostatic charge constant  $d_h$ .

## V. SUMMARY AND DISCUSSION

Attempts were made to produce 1-3 composites in which both polymer and ceramic phases are piezoelectric in anticipation to obtain enhanced piezoelectric activity from the

composite. The polymer used was a VDF/TrFE copolymer and was added to the ceramic using both the layering and dice-and-fill techniques. The former method was a reliable way of producing composites, but is difficult to use for com-

TABLE III. Piezoelectric coefficients of 75/25 mol % VDF/TrFE copolymer measured at 80 Hz.

Sample	Poling field (kV mm <sup>-1</sup> )	$d_{33}$ (pC N <sup>-1</sup> )	$d_h$ (pC N <sup>-1</sup> )
Solvay film	51	-29.6 ± 0.5	-11.0 ± 0.5
Solvay film	36	-19 ± 2	-7.0 ± 0.5
Cast from acetone	26	-7 ± 0.5	-6.0 ± 0.5
Cast from acetone	15	-6.0 ± 0.4	-2.0 ± 0.1

posites with a small periodicity. The dice-and-fill technique was also used and in this case the copolymer was dissolved in acetone and cast in grooves which were cut in the ceramic. This method leads to difficulties with breakage of the fine ceramic rods, due to shrinkage of the polymer, and the yield was low. Melting the polymer into the grooves of a diced ceramic does not appear to be a viable alternative, because of the high viscosity of the melted polymer. Both the layered and the dice-and-fill samples proved difficult to pole due to breakdown at the polymer/ceramic interface. This is probably the major problem to be overcome if this type of composite is to achieve its potential.

Modeling and measurement results are in reasonable agreement with the exception of the piezoelectric coefficient  $d_h$ . The fact that the measured  $d_h$  is much lower than predicted, while  $k_t$  is not, is somewhat anomalous. If the low  $d_h$  was due to inadequate poling, it would be expected that both  $d_h$  and  $k_t$  would be low. A possible explanation is that the results are a consequence of the frequency of measurement. As described,  $d_h$  is measured at 80 Hz, while  $k_t$  comes from measurements on a resonance peak at around 1 MHz. Since the piezoelectric materials are effectively capacitive sources, any leakage resistance through them will form a high-pass filter for the piezoelectric voltage. This may affect the measured  $d_h$  values and have less effect on  $k_t$ . Such leakage

resistance could result from the same sources which lead to breakdown during the poling of the composites and would be evident in the composites, but not in the pure copolymer or ceramic.

## ACKNOWLEDGMENTS

The authors would like to acknowledge the support from the CSIRO/Macquarie University Collaborative Project Fund. Thanks are also due to I. Paterson and the Macquarie University workshop for their help.

- <sup>1</sup>H. Takeuchi and C. Nakaya, *Ferroelectrics* **68**, 53 (1986).
- <sup>2</sup>A. A. Shaulov, U. S. Patent No. 4,671,293 (1987).
- <sup>3</sup>R. Y. Ting, *Ferroelectrics* **67**, 143 (1987).
- <sup>4</sup>H. L. W. Chan and I. L. Guy, in *Ferroelectric Polymers and Ceramic-Polymer Composites*, edited by D. K. Das-Gupta (Trans Tech, Zürich, 1994).
- <sup>5</sup>M. Latour and R. L. Moreira, *IEEE Trans. Electron. Insul.* **EI-21**, 525 (1986).
- <sup>6</sup>W. A. Smith, in *Proceedings of the 1989 IEEE Ultrasonics Symposium* (IEEE, New York, 1990), p. 757.
- <sup>7</sup>H. P. Savakus, K. A. Klicker, and R. E. Newnham, *Mater. Res. Bull.* **16**, 677 (1981).
- <sup>8</sup>J. Zola, U.S. Patent No. 4,514,247 (1985).
- <sup>9</sup>H. Taunamang, I. L. Guy, and H. L. W. Chan, in *Proceedings of the International Symposium on Polymer and Composites*, Hong Kong, 1992.
- <sup>10</sup>P. D. Southgate, *Appl. Phys. Lett.* **28**, 250 (1976).
- <sup>11</sup>B. Hartmann, *Methods of Experimental Physics* (Academic, New York, 1980), Vol. 16C, p. 59.
- <sup>12</sup>IEEE Standard on Piezoelectricity, *IEEE Std.* 176, 1978.
- <sup>13</sup>R. H. Tancrell, D. T. Wilson, and D. Ricketts, in *Proceedings of the 1985 IEEE Ultrasonics Symposium* (IEEE, New York, 1985), p. 624.
- <sup>14</sup>H. Taunamang, M.S. thesis, Macquarie University, NSW, Australia, 1993.
- <sup>15</sup>Data sheets from GEC-Marconi, 1992.
- <sup>16</sup>H. Ohigashi and K. Koga, *Jpn. J. Appl. Phys.* **21**, L455 (1982).
- <sup>17</sup>H. Ohigashi, *J. Appl. Phys.* **47**, 949 (1976).
- <sup>18</sup>Vernitron data sheet, 1988.
- <sup>19</sup>H. Jaffe and D. A. Berlincourt, *Proc. IEEE* **53**, 1372 (1965).
- <sup>20</sup>I. L. Guy and J. Unsworth, *Appl. Phys. Lett.* **52**, 532 (1988).

Journal of Applied Physics is copyrighted by the American Institute of Physics (AIP). Redistribution of journal material is subject to the AIP online journal license and/or AIP copyright. For more information, see <http://ojps.aip.org/japo/japcr/jsp>  
Copyright of Journal of Applied Physics is the property of American Institute of Physics and its content may not be copied or emailed to multiple sites or posted to a listserv without the copyright holder's express written permission. However, users may print, download, or email articles for individual use.